Soil & Tillage Research 231 (2023) 105716

Contents lists available at ScienceDirect

Soil & Tillage Research

journal homepage: www.elsevier.com/locate/still

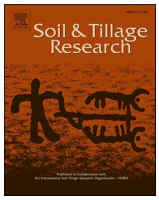

Assessing the effects of agricultural management practices and land-use changes on soil organic carbon stocks

Qingwei Zhuang [a], Zhenfeng Shao [a,*], Lu Kong [b,c], Xiao Huang [d], Yuzhen Li [e], Yuyan Yan [b,c], Shixin Wu [b]

[a] State Key Laboratory of Information Engineering in Surveying, Mapping and Remote Sensing, Wuhan University, Wuhan 430079, China
[b] State Key Laboratory of Desert and Oasis Ecology, Xinjiang Institute of Ecology and Geography, Chinese Academy of Sciences, Urumqi 830011, China
[c] University of Chinese Academy of Sciences, Beijing 100049, China
[d] Department of Geosciences, University of Arkansas, Fayetteville, AR 72701, USA
[e] School of Emergency Management, Xihua University, Chengdu 610039, China

ARTICLE INFO

Keywords:
Soil organic carbon
Land-use changes
Agricultural management practices
Arid regions

ABSTRACT

Soil organic carbon (SOC) stocks have profound effects on climate change, sustainable agricultural development, and environmental management. Our objectives were to propose a conceptual framework and quantify the impact of land use change (LUC) and agricultural management practices (AMPs) on SOC stocks. By comparison, we choose the Kriging-based spatial prediction model to estimate SOC stocks based on the field sampled soil data (depth of 0–30 cm) in 2005 and 2019. Film mulching, drip irrigation, and fertilizer application were selected to represent the regional AMPs. Our results indicate that SOC stocks increased by 12.7% in the Sangong river basin from 2005 to 2019. From the proposed conceptual framework, we notice that the transition between different land-use types may cause both losses (e.g., −9.49 Gg C caused by expansion of construction land) and gains (e.g., +3 Gg C caused by the conversion of cultivated land to grassland) of SOC storage. Benefiting from improved AMPs (e.g., film mulching, drip irrigation, and fertilizer application), the "stable cultivated land" category contributes the most (+36.0 Gg C) to the growth of SOC stocks.

1. Introduction

Soil organic carbon (SOC) pool is the largest terrestrial reservoir of carbon (C) (Carvalhais et al., 2014), approximately twice the atmospheric C pool and about three times the terrestrial vegetation C pool (Dlamini et al., 2016). The fixation of atmospheric carbon by increasing the SOC pool is particularly important for mitigating the greenhouse effect and has become a hot spot and focus of current research in the field of climate change (Balesdent et al., 2018; Bradford et al., 2016). In farmland ecosystems, the SOC stocks decreases with increasing soil depth (Xie et al., 2007; Xu et al., 2011). Numerous investigations have been made on surface SOC with a focus on land use change (LUC) or agricultural management practices (AMPs) (Ramirez et al., 2020; Mbuthia et al., 2015; Sanderman et al., 2017; Wiesmeier et al., 2019; Bai et al., 2018). Most of the existing studies investigated the effect of LUC on SOC stocks (Don et al., 2011; Franco et al., 2020; Ren et al., 2020). A small number of existing studies investigated the effects of AMPs on SOC stocks (Baker et al., 2007; Dignac et al., 2017; Zhang et al., 2021). However, no existing study was designed to explore the combined effects of AMPs and LUC on SOC stocks under the same framework. Hence, this study is critical for the agriculture and climate change communities to explore the combined effects of AMPs and LUC on SOC stocks by designing a conceptual framework."

Agricultural soil is subject to frequent anthropogenic disturbance during development, resulting in a stronger spatial variability of SOC than natural soils (Bai et al., 2020; Crystal-Ornelas et al., 2021; Bouasria et al., 2022). High-precision prediction of the spatial distribution of SOC stocks in agricultural soil is much more difficult than that in natural soils. As to now, the methods for predicting SOC stocks can be classified into 4 categories: (1) Soil type linkage method based on soil properties (Wu et al., 2018); (2) Geostatistical methods, such as inverse distance weighting (IDW), Tyson polygons, etc. (Nandan et al., 2019); (3) Multiple linear regression method (Huang et al., 2015); (4) Machine learning methods, e.g., random forests (RF), support vector machines (SVM), decision trees, etc (Guo et al., 2021; Keskin et al., 2019; Morais et al., 2020). The soil type linkage method is suitable for areas with large

* Corresponding author.
E-mail address: shaozhenfeng@whu.edu.cn (Z. Shao).

https://doi.org/10.1016/j.still.2023.105716
Received 7 August 2021; Received in revised form 24 March 2023; Accepted 31 March 2023
Available online 11 April 2023

spatial scales and relatively homogeneous soil types, but it does not reflect enough of the diversity of soil types (Lemma et al., 2021). The geostatistical method relies more on spatial correlation, and its ability to express spatial characteristics and prediction accuracy is poor in areas with complex scenarios and strong local variability (Lal, 2018). Multiple linear regression has a poor ability to characterize the nonlinear spatial distribution of SOC stocks (Bouasria et al., 2022). The prediction accuracy of the machine learning algorithm model is strongly dependent on the spatial scale and sampling density, and the measurement error is huge in large-scale complex scenarios (Zhang et al., 2020). Therefore, the existing method needs to be improved to enhance the estimation accuracy.

Existing studies have proved that LUC is one of the most important factors for SOC stocks (Artemyeva et al., 2021; Bai et al., 2020; Lizaga et al., 2019; Wang and Zhao, 2020). At the same time, changes in different land use types also affect the SOC storage, SOC components, and C cycle mechanisms (Li et al., 2022; Xiao et al., 2021; Xu et al., 2022; Zhuang et al., 2022a). The positive or negative impact depends on the land use types before and after the changes. Among them, some conversion between different land use types (e.g., forests to cultivated land, cultivated land to construction land, etc.) may destabilize the aggregate stability of the soil, leading to a decreased impact on SOC stocks (Fujisaki et al., 2015; Liu et al., 2020; Li et al., 2021). The excessive disturbance caused by land use change (e.g., grassland to barren land, grassland to cultivated land, cultivated land to industrial and mining land, etc.) may increase soil erosion. The horizontal migration of SOC that occurs during soil erosion can significantly alter the distribution pattern of SOC in terrestrial ecosystems (Franco et al., 2020; Damian et al., 2021; Zhang et al., 2021). Therefore, investigations on the impact of LUC on SOC stocks are in great need and can provide important guidance to the formation of major ecological policies and land resource allocation.

This discovery has brought more attention to the importance of AMPs in regulating the C storage and C cycle of terrestrial ecosystems (Cooper et al., 2021; Sanaullah et al., 2020; Zhuang et al., 2022b). AMPs change SOC by affecting soil conditions (Dignac et al., 2017). He et al. (2021b) pointed out that different agronomic management plans have different effects on the distribution and stability of aggregation. For example, as the tillage intensities increase, SOC reserves decrease. In recent years, the AMPs in arid regions have undergone tremendous changes (Fu et al., 2015; Ming et al., 2021), mainly reflected in three aspects: 1) mulching farming, 2) drip irrigation, and 3) fertilizer application (Zhao et al., 2021). However, few efforts have been made to explore the comprehensive impact of these several AMPs on SOC stocks. The response mechanisms of AMPs to SOC stocks under the background of drastic LUC are largely unknown.

If the effects of LUC and AMP on SOC were not explored clearly, it will be detrimental for administrators to improve the quality of cropland and enhance soil carbon sink. To fill the gap, we explore the combined effects of LUC and AMPs on SOC stocks in arid regions. The Sangong

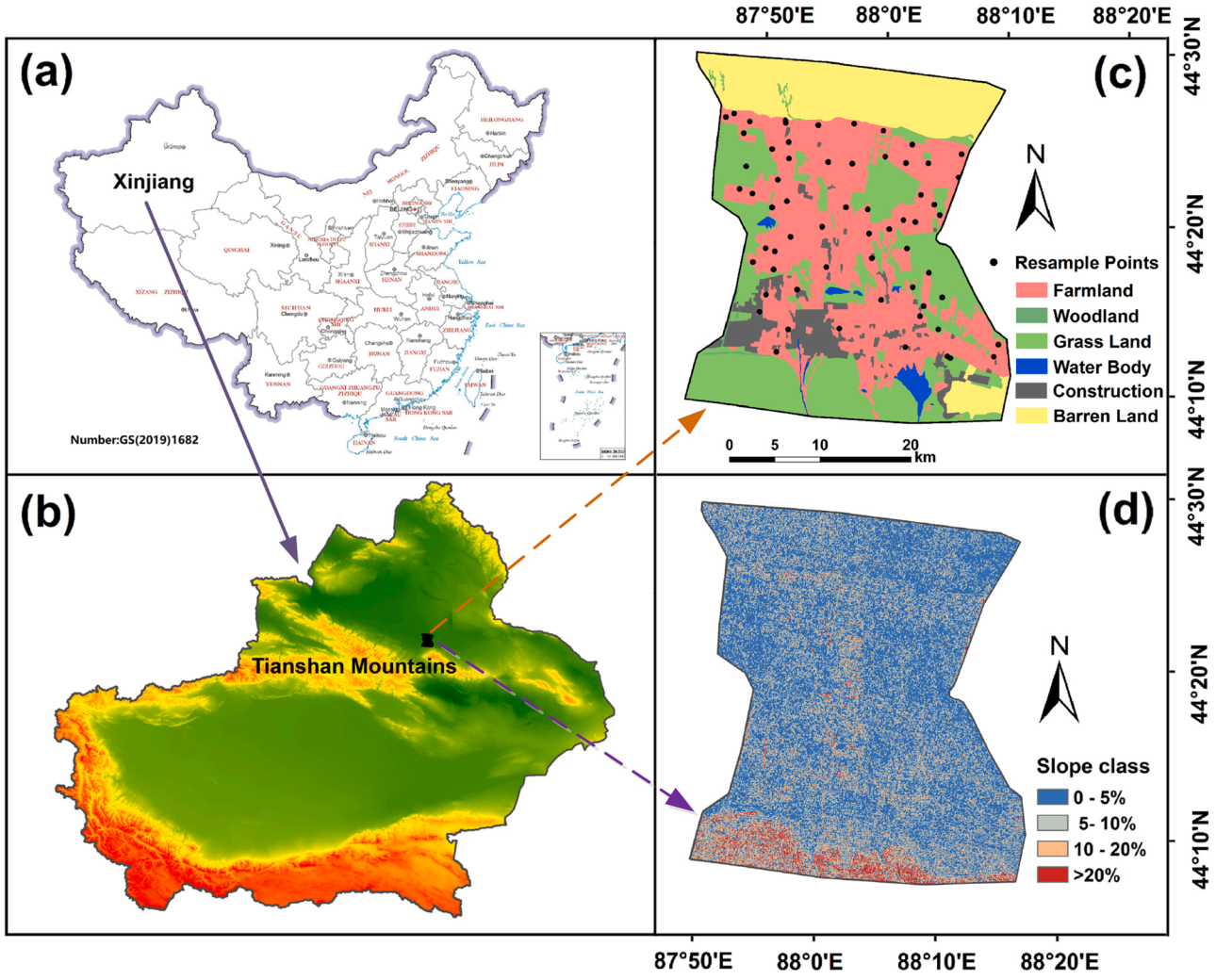

Fig. 1. **(a)** Location of Xinjiang Province in China (Boundary information was obtained from the Ministry of Natural Resources of China, Approve number: GS(2019) 1682); **(b)** Location of the Sangong river basin in Xinjiang; **(c)** distribution of sampling points in the study area in 2019; and **(d)** slope map of the study area

river basin is chosen as the study area as it is a typical arid region characterized by the rapid transformation of agricultural management patterns and a large-scale farmland expansion (Hou et al., 2011). We improved the Kriging-based spatial prediction model to estimate SOC stocks based on the field sampled soil data (depth of 0–30 cm) in 2005 and 2019 and propose a conceptual framework to quantify the impact of land use change (LUC) and agricultural management practices (AMPs) on SOC stocks.

2. Materials and methods

2.1. Study area and soil sampling

The Sangong river basin in Xinjiang, China, is characterized by the landform pattern of mountain-plain-river-desert at 43°09′N–45°29′N and 87°47′E–88°17′E (Fig. 1). The area of cultivated land has increased from 96.4 km^2 in 1949–680 km^2 in 2019. It has a typical temperate continental climate, with the average annual temperature (1990–2018) greatly differing among different geomorphic units: 2.54 °C in the mountainous area, 6.62 °C in the central plain, and 7.21 °C in the northern desert area. The average annual precipitation of the whole basin is about 200 mm. The inter-annual variation of precipitation is relatively large, ranging from 100 mm to 340 mm. The average annual evaporation of this basin is about 1800 mm, where the northern desert presents 500 mm greater in average annual evaporation than that of the southern mountain area. The average annual runoff of surface water is 9.84×10^7 m^3, mainly coming from alpine glaciers and snowmelt. The surface water varies within a year, with summer runoff accounting for 75% of the total runoff and spring runoff accounting for only 15%.

According to soil types, vegetation types, and cultivated land reclamation period, we arranged representative cultivated land sampling points on the high-resolution topographic map and selected a total of 62 representative sampling points in the Sangong river basin (Fig. 1c). The soil samples were collected in May 2005 and May 2019. When sampling, the ridge roadsides, ditches, and micro-topography were avoided. A composite soil sample from each plot was collected by combining six randomly collected cores from soybean inter-row from 0 − 30 cm depth using a bucket-type auger of 5 cm diameter. The specific information of 62 sampling points can be found in Table S1.

2.2. Bulk soil analysis

The content of SOC was determined by the "potassium dichromate oxidation-external heating" method (Mazzoncini et al., 2011). First, 0.5 g sample was weighed and put into a hard test tube, and 0.1 g silver sulfate and 5 mL potassium dichromate standard solution (with pipette) were added. Then 5 mL concentrated sulfuric acid with a syringe was added and carefully rotated and shaken. The oil pan was heated to 185 °C − 190 °C in advance, and the hard test tube with the sample was inserted into the wire cage rack and then put into the oil pan for heating. The temperature in the oil pan was controlled at 170 °C − 180 °C while the solution was kept boiling for 5 min. Finally, we took out the wire cage frame and put it in the test tube frame when the test tube was cooled. The solution with green color suggests that the amount of potassium dichromate is insufficient and should be redone. If the color of the solution is orange-yellow or yellow-green, we pour the digestion liquid in the test tube into a 150 mL Erlenmeyer flask. Then four drops of the o-phenanthroline indicator were added and titrated the remaining potassium dichromate with 0.2 mol/L ferrous ammonium sulfate standard solution. We recorded the volume of ferrous ammonium sulfate solution when the color of the solution changed from orange-yellow to brownish-red.

$$W_{soc} = 0.800 \times 5.0/V_0 \times (V_0 - V) \times 0.003 \times 1.10 \times m \quad (1)$$

where W_{SOC} is the amount of SOC per unit weight of soil (g); 0.800 is the concentration of potassium dichromate standard solution (mol/L); 5.0 is the volume of potassium dichromate standard solution (mL); V_0 is the volume of $Fe(NH_4)_2{\cdot}(SO_4)_2{\cdot}6\ H_2O$ standard solution consumed by blank (mL); V is the volume of $Fe(NH_4)_2{\cdot}(SO_4)_2{\cdot}6\ H_2O$ standard solution consumed by the sample (mL); 0.003 is the mill molar mass of 1/4 carbon atom (g); 1.10 represents the oxidation correction coefficient; m is the weight of the sample (g).

2.3. Estimation of SOC stocks

SOC density refers to the quantity of SOC in a certain depth of soil per unit area. It is calculated by the following formula:

$$D_{oc} = S_{oc} \times \gamma \times H \times 10^{-3} \quad (2)$$

where D_{oc} is the SOC density ($kg.m^{-2}$); S_{oc} is the SOC content ($g.kg^{-1}$); γ is the soil bulk density ($g.cm^{-3}$), determined by the ring knife method; H = 30 cm, which is the depth of surface soil in this study.

The soil bulk density (γ) was measured by the Cutting Ring Method (Jiang, 2019). Soil γ is calculated by the formula:

$$\gamma = \frac{m \times 100}{V \times (100 + W)} \quad (3)$$

where V is the volume of the ring knife (cm^3); m is the weight of wet soil inside the ring knife (g); W is the water content of soil weight inside the ring knife (%).

Further, we use the soil type method to estimate the surface SOC stocks (Lal, 2018). The formula is as follows:

$$P_{oc} = \sum_{i=1}^{n} S_i \times D_{oci} \quad (4)$$

where P_{oc} is the surface SOC stocks (Gg C); S_i is the area of the i^{th} soil patch (hm^2); D_{oci} is the carbon content of the i^{th} soil patch (Gg C/hm^2); n is the total number of patches.

2.4. Kriging-based spatial prediction model for SOC stocks

To improve the prediction accuracy, we introduce collaborative regionalization variables on the basis of the Kriging spatial prediction model. Collaborative regionalization variables refer to variables that have spatial and statistical correlations in the same spatial range (Yang et al., 2020). This study uses regression Kriging under the digital surface model (DSM) to create a spatial prediction map of SOC stocks. The accuracy of spatial prediction results can be improved based on the correlation between collaborative variables and SOC. The uncertainty test of the prediction results is carried out according to the standards stipulated by the GlobalSoilMap (GSM) project, which defines the uncertainty as the 95% prediction interval (PI): the true value is expected to occur 9 times out of 10, with a 1 out of 20 probability for each of the two tails. Reliable spatial prediction results of SOC stocks are expected to better benefit subsequent analysis (Shi et al., 2016). The co-Kriging prediction formula of three variables is as follows:

$$SOC_{3,ck}(x_0) = \sum_{i=1}^{n_1} \lambda_{1i} Z_1(x_{1i}) + \sum_{j=1}^{n_2} \lambda_{2j} Z_2(x_{2j}) + \sum_{k=1}^{n_3} \lambda_{3k} Z_3(x_{3k}) \quad (5)$$

where $SOC_{3,ck}(x_0)$ is the predicted SOC stocks at the sampling point; λ_{1i} represents the weight of the sampling points involved in the prediction to the SOC stocks of the sampling points; $Z_1(x_{1i})$ refers to the measured value of SOC stocks at sampling point; λ_{2j} is the weight of elevation involved in the prediction to the SOC stocks; $Z_2(x_{2j})$ represents the measured value of elevation; λ_{3k} refers to the weight of slope or DSM involved in the prediction to the SOC content; $Z_3(x_{3k})$ represents the measured value of the slope or DSM; n_1, n_2, and n_3 indicates the number of soil sampling points, elevation sampling points, and slope sampling

points, respectively.

2.5. Accuracy evaluation

In order to verify and compare the results of different forecasting methods, we use the cross-validation method to judge the performance of each forecasting model. The principle of the cross-validation method is to use the points around each measured point to predict the measured value, and compare the predicted value with the measured value itself (Nocita et al., 2014). In this paper, we use the mean absolute error (MAE) and root mean square error (RMSE) to evaluate the accuracy of the prediction results:

$$MAE = \frac{1}{n}\sum_{i=1}^{n}|Z(x_i) - Z'(x_i)| \quad (6)$$

$$RMSE = \sqrt{\frac{1}{n}\sum_{i=1}^{n}[Z(x_i) - Z'(x_i)]} \quad (7)$$

where $Z(x_i)$ represents the measured value; $Z'(x_i)$ refers to the predicted value; n is the number of verification points.

2.6. A conceptual framework for exploring the joint impact of land-use changes and agricultural management practices on SOC stocks

In this study, we propose a conceptual framework to explore the impact of land-use changes and agricultural management practices on the SOC stock. The proposed framework separates the impacts into contributions of land-use change (*Contr.Luc*), agricultural management practices (*Contr.Amp*), and residual factors (*Contr.Res*). We adopt a total least squares optimal fingerprinting approach that uses a generalized linear regression model to represent observed changes as a linear combination of signals. *Contr.Luc* represents the impact of the conversion between land use types. *Contr.Amp* induced by several agricultural management patterns (e.g., film mulching, drip irrigation, and fertilizer application) may promote or inhibit SOC stocks. In addition, the SOC stocks may be affected by other factors (e.g., crop species, planting system, etc.), which are captured by *Contr.Res* that represents the contribution of residual factors to the SOC stocks.

$$\Delta SOC_{\mathrm{p}} = Contr.Luc + Contr.Amp + Contr.\mathrm{Res} \quad (8)$$

where ΔSOC_{p} is the anomaly of the sequestration potential of SOC from 2005 to 2019; *Contr.Luc*, *Contr.Amp*, and *Contr.Res* are the variations of SOC stocks caused by land-use changes, agricultural management practices, and residual factors.

During the investigated period, the land use in the Sangong river basin has undergone drastic changes, with the area of cultivated land expanding rapidly. Meanwhile, the loss of cultivated land was notable, presumably due to urban expansion. To explain the impact of land-use changes on the SOC stocks, we divide this process into two parts (Eq. 9).

$$Contr.Luc = \Delta SOC_{p-crop-others} + \Delta SOC_{p-others-crop} \quad (9)$$

where $\Delta SOC_{p-crop-others}$ is the dynamics of SOC stocks caused by the conversion of other land use types to cultivated land; $\Delta SOC_{p-others-crop}$ refers to the dynamics of SOC stocks due to the conversion of cultivated land to other land use types.

Agricultural management practices affect the SOC stocks in the farmland ecosystem. Long-term cropping system experiments offer a great opportunity to understand the magnitude and direction of the sequestration potential change of SOC. In recent decades, the changes in agricultural management practices are mainly reflected in mulching planting, drip irrigation technology, and fertilizer application per unit area:

$$Contr.Amp = Contr.Mulch + Contr.Drip + Contr.Fertilization \quad (10)$$

$$Contr.Mulch = SOC_{p-post-mulch} - SOC_{p-pre-mulch} \quad (11)$$

$$Contr.Drip = SOC_{p-post-drip} - SOC_{p-pre-drip} \quad (12)$$

$$Contr.Fertilization = SOC_{p-post-fertilization} - SOC_{p-pre-fertilization} \quad (13)$$

where *Contr.Mulch*, *Contr.Drip*, and *Contr.Fertilization* are the contributions of mulching planting, drip irrigation technology, and fertilizer application per unit area to the shift of SOC stocks, respectively; $SOC_{p\text{-}post\text{-}mulch}$ and $SOC_{p\text{-}pre\text{-}mulch}$ are the average SOC_p within the post-mulch and pre-mulch periods, respectively; $SOC_{p\text{-}post\text{-}drip}$ and $SOC_{p\text{-}pre\text{-}drip}$ represent the average SOC_p within the post-drip irrigation and pre-drip irrigation periods, respectively; $SOC_{p\text{-}post\text{-}fertilization}$ and $SOC_{p\text{-}pre\text{-}fertilization}$ denote the average SOC_p within the post-fertilization and pre-fertilization periods, respectively.

3. Results

3.1. Data quality

SOC ranges from 0.929 g/kg to 21.7 g/kg in 2005. The average content of SOC in 2005 with 62 resample points is 7.16 g/kg (Table 1). In 2019, the average SOC is 8.20 g/kg, with an increase of 1.05 g/kg compared to 2005. In this study, we estimated the heterogeneity of variables based on the coefficient of variation (CV). The CV value indicates that the SOC data of the two periods are of moderate variation (50.8% in 2005 and 52.4% in 2019). According to the joint test of skewness and kurtosis, the surface SOC content in 2005 and its logarithm in 2005 conform to the normal distribution. In comparison, the surface SOC content in 2019 does not conform to the normal distribution, but its logarithm conforms to the normal distribution. These results indicate the SOC data for 2005 and 2019 can be spatially interpolated via the Kriging-based model.

3.2. Estimation, distribution, and dynamics of SOC stocks in 2005 and 2019

According to the spatial estimation results, Fig. 2a and Fig. 2b show the spatial distribution patterns of surface SOC content in the Sangong river basin in 2005 and 2019, respectively. In 2005, the SOC content ranged from 0.158 $kg.m^{-2}$ to 1.38 $kg.m^{-2}$, with an average level of 0.473 $kg.m^{-2}$. The highest SOC stocks occurred in the southeast of the study area with a high elevation and abundant precipitation. In contrast, the lowest SOC stocks occurred in the northeast and west study area under a dry climate covered by barren land(Fig. 2a). The SOC content fluctuated in the range of 0.168 $kg.m^{-2}$ to 1.338 $kg.m^{-2}$, with an average level of 0.533 $kg.m^{-2}$ in 2019. The highest SOC stocks occurred in the central and southeast Sangong River Basin, covered by farmland and with relatively complete water conservancy facilities. In comparison, the lowest SOC stocks were concentrated in the northeast and northwest study area covered by barren land (Fig. 2b).

In general, the surface SOC content had seen a notable increase from 2005 (0.473 $kg.m^{-2}$) to 2019 (0.533 $kg.m^{-2}$) in the study area. It can be seen from Fig. 2c that areas where the surface SOC content decreases are mainly distributed in the eastern part of the Sangong river basin, accounting for about 25.5% of study area. The areas where the surface SOC content increased mainly occurred in the central and western of the study area, accounting for approximately 74.5% of the area of the study area. From 2005–2019, the surface SOC storage in the Sangong river basin increased by 50 Gg C (524 Gg C in 2005, 574 Gg C in 2019, 1 Gg C = 10^9 g C), a net increase of 9.5%. The detailed reasons are discussed in Sections 3.3 and 3.4.

Table 1
SOC content of the surface soil (0–30 cm) in 2005 and 2019.

Year	Parameter	Minimum (g/kg)	Maximum (g/kg)	Average (g/kg)	Standard Deviation	Coefficient of Variation (%)	Skewness	Kurtosis
2005	SOC	0.929	21.7	7.16	3.63	50.8	0.659	0.317
	Logarithm of SOC	-0.032	1.34	0.791	0.250	31.6	-0.181	0.483
2019	SOC	2.57	21.1	8.20	4.30	52.4	0.836	0.216
	Logarithm of SOC	0.410	1.32	0.853	0.233	27.3	-0.078	-0.666

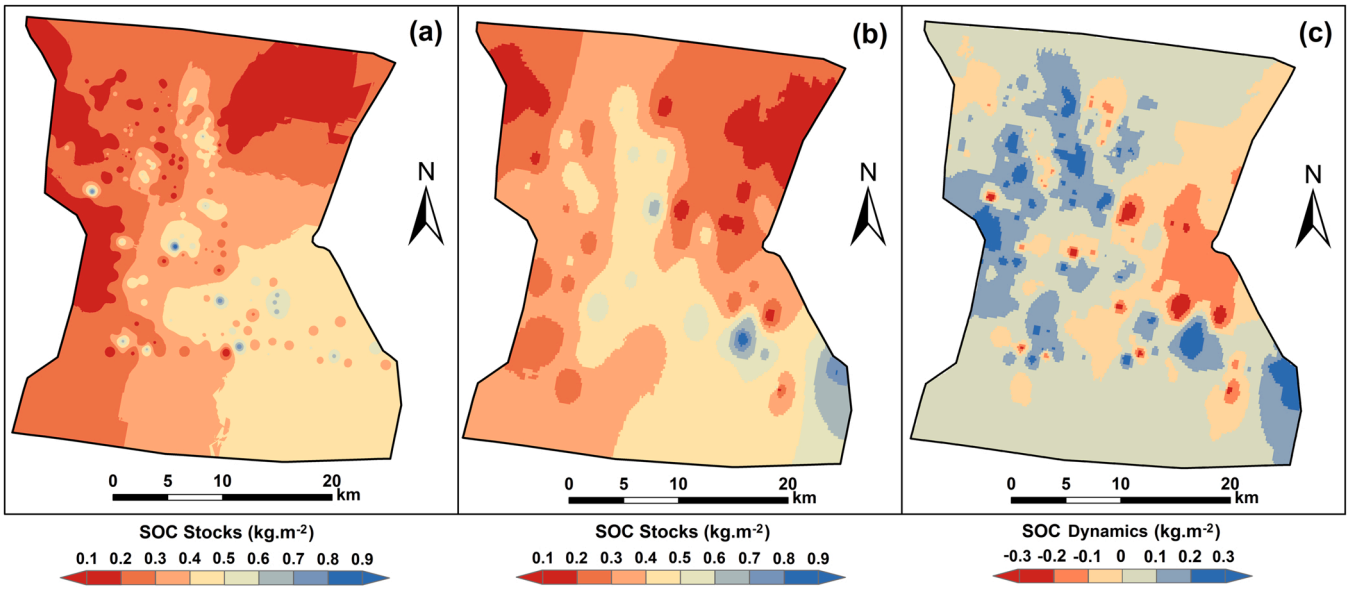

Fig. 2. Distribution of SOC content in 2005 **(a)**, 2019 **(b)**, and the dynamics of SOC content from 2005 to 2019 **(c)**.

3.3. Contribution of land-use change to SOC stocks

The spatial-temporal distribution of each land use type in 2005 (Fig. 3a), 2010 (Fig. 3b), 2015 (Fig. 3c), and 2019 (Fig. 3d) is presented. The transfer matrix of land use patterns was obtained by overlaying the land use dataset from 2005 to 2019 (Table 2). The statistical results show that land use patterns have undergone tremendous changes. We noticed two phenomena. First, cultivated land encroached a large amount of grassland (103 km^2), accounting for 99.5% of the increased cultivated land during 2005–2019. This phenomenon can be explained by the pressure of population and agricultural economy, potentially bringing huge challenges to water resources and environmental security in arid regions. Second, the area of cultivated land has decreased by 37.1 km^2, with 41.9% of them converted into construction land (Table 2). These cultivated land were found concentrated around the urban fabric, suggesting that the process of urbanization poses a serious threat to farmland quality and food security. In addition, 21.4 km^2 of cultivated land was converted into grassland, accounting for 57.8% of the lost cultivated land. This phenomenon is caused by fallow and responding to the government's policy of "returning cultivated land to woodland and grassland". The above results revealed the important role of human activities in driving the changes in land use patterns.

In 2005, the order of SOC pool of each land use type follows: grassland (211 Gg C) > cultivated land (196 Gg C) > barren land (78.1 Gg C) > construction land (16.2 Gg C). The order of SOC pool for each land cover type in 2019 follows: cultivated land (278 Gg C) > grassland (186 Gg C) > barren land (90.1 Gg C) > construction land (27.5 Gg C) > woodland (1.54 Gg C). Among them, the surface SOC of stable cultivated land received the most increased amount by 36.0 Gg C (Table 3). The surface SOC in stable grassland and stable barren land increased by 18.6 Gg C and 13.4 Gg C, respectively. The surface SOC of stable construction land decreased by 1.05 Gg C during the investigated period. Compared with stable land use types, the mutual conversion between different land use types is expected to have more complex effects on surface SOC stocks. The conversion of grassland to construction land (−4.77 Gg C) and cultivated land to construction land (−4.54 Gg C) caused the highest SOC loss among all land-use conversions. Meanwhile, the conversion of cultivated land to grassland (+3 Gg C) also has a positive impact on SOC stocks. In contrast, the conversion of grassland to cultivated land led to the decrease of surface SOC stocks by 10.1 Gg C.

3.4. SOC stocks of cultivated land in response to agricultural management practices

It can be seen from Table 3 that the decreased cultivated land caused a large amount of surface SOC loss (−7.56 Gg C). The above results also confirm that land use changes are one of the important reasons for changes in soil C sources and C sinks. What surprised us is the fact that the shallow SOC of the stable cultivated land in the Sangong river basin increased by 36 Gg C (177 Gg C in 2005 and 213 Gg C in 2019) from 2005 to 2019, a relative increase of 20.4%. In most cases, stable cultivated land is hardly affected by land-use changes. Therefore, we further explored the impact of agricultural management practices on surface SOC stocks from three aspects, i.e., film mulching rate, drip irrigation, and fertilizer application. First, the film mulching rate in our study area increased from 31.1% in 2005 to 60.1% in 2019. Plastic film mulching has a highly promoting effect on the stability of surface soil aggregates. Aggregates are the main place where organic carbon exists, and the improvement of its stability is beneficial to SOC stocks (Nabiollahi et al., 2018). Second, changes in soil moisture content and distribution caused by changes in irrigation methods can also be responsible for the increase of SOC stocks (Qiu et al., 2022). In 2019, the area of drip irrigation farmland accounted for 58.7% of the total farmland, while this number was only 40.1% in 2005. Third, it is widely recognized that reducing the usage of chemical fertilizer and increasing fertilizer efficiency can promote SOC stocks. The fertilizer application in the Sangong river basin

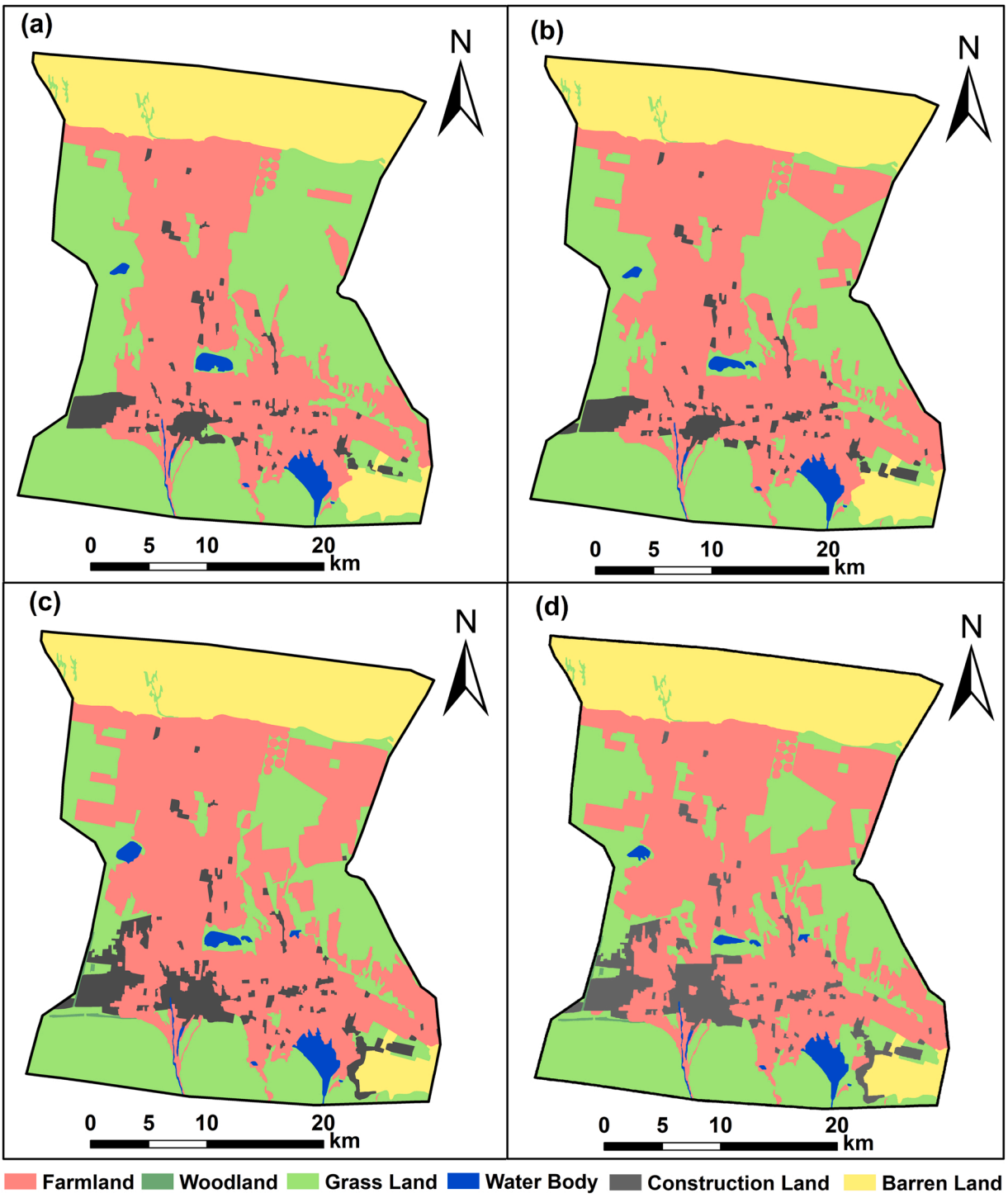

Fig. 3. Distribution of land use types in 2005 **(a)**, 2010 **(b)**, 2015 **(c)**, and 2019 **(d)**.

decreased from 252 kg/hm^2 to 175 kg/hm^2 during the investigated time period. The reduction of fertilizer application enhances the soil carbon sequestration capacity by reducing the cumulative mineralization amount and cumulative mineralization rate of SOC. From the above analysis, we believe that the increase in film mulching rate, the increase of drip irrigation area, and the reduction of fertilizer application jointly promoted the increase in surface SOC stocks in our study area.

4. Discussion

4.1. Verification and uncertainty of estimation results

This study optimizes the spatial prediction of SOC content via the Kriging-based model to select variables and assess the uncertainty of the forecast results. The Kriging-based gives the model parameters based on the covariates with the highest confidence and provides a measure of uncertainty. The prediction statistics indicate low uncertainty in the training dataset in 2005 and 2014 (significance level at 0.01) (Table 4). The RMSE (0.65 in 2005 and 0.67 in 2019) and MAE (0.39 in 2005 and

Table 2
Transfer matrix of land use patterns between 2005 and 2019 (km^2).

Year	Patterns	2019							
		WOO	GRA	WAT	CON	BAR	CUL	Total	Decrease
2005	WOO	0	0	0	0	0	0	0	0
	GRA	2.84	326	1.13	14.0	0	103	447	121
	WAT	0	2.48	13.6	0	0	0	16.1	2.48
	CON	0.01	0	0	29.7	0	0.52	40.2	0.53
	BAR	0	0	0	3.70	213	0	217	3.70
	CUL	0	21.4	0.14	15.5	0	333	370	37.1
	Total	2.85	350	14.9	72.9	213	436	1090	\
	Increase	2.85	23.9	1.27	33.2	0	103	\	\

Note: WOO, woodland; GRA, grassland; WAT, water body; CON, construction land; BAR, barren land; CUL, cultivated land.

Table 3
Mean absolute and relative SOC stocks changes for different land-use change types.

Land-use change types	SOC density (kg/m^{-2})		Area (km^2)	SOC stocks (Gg)		SOC dynamics (Gg)
	2005	2019		2005	2019	
Stable GRA	0.47	0.53	326	153	173	19.6
Stable CON	0.40	0.37	39.7	15.9	14.7	-1.19
Stable BAR	0.36	0.42	213	76.7	89.5	12.8
Stable CUL	0.53	0.64	333	177	213	36.6
GRA to WOO	0.45	0.54	2.84	1.28	1.53	0.26
GRA to CON	0.67	0.33	14.0	9.38	4.62	-4.76
GRA to CUL	0.46	0.56	103	57.5	47.2	-10.3
BAR to CON	0.42	0.37	3.70	1.55	1.37	-0.19
CUL to GRA	0.66	0.52	21.4	11.2	14.2	3.00
CUL to CON	0.64	0.34	15.5	9.95	5.28	-4.66
Other types	2.40	2.35	4.28	10.3	10.0	-0.24
Study area	0.47	0.53	1077	524	574	50

Note: WOO, woodland; GRA, grassland; CON, construction land; BAR, barren land; CUL, cultivated land.

Table 4
Performance of the Kriging-based model to predict the spatial distribution of SOC content.

Year	Dataset Types	R^2	PCC	RMSE	MAE	n
2005	Training Dataset	0.967	0.983**	0.65	0.39	42
	Validation Dataset	0.814	0.705**	2.38	1.42	20
2019	Training Dataset	0.956	0.978**	0.67	0.41	42
	Validation Dataset	0.755	0.673**	2.71	1.67	20

Note: PCC, Pearson Correlation Coefficient; RMSE, Root Mean Squared Error; MAE, Mean Absolute Error.

0.41 in 2019) corroborate this assertion, presenting small differences in 2005 and 2019. Compared with the training dataset, the RMSE (2.38 in 2005 and 2.71 in 2019) and MAE (1.42 in 2005 and 1.67 in 2019) in the validation dataset show greater changes, indicating increased uncertainty in the prediction results have increased (significance level at 0.01), which can be explained by the small number of samples used for verification. Table 5.

Table 5
Comparison of prediction models using the validation data in 2019.

Models	R^2	PCC	MAE	RMSE
IDW	0.573	0.491*	3.52	4.38
Spline	0.661	0.575*	2.74	3.86
SVM	0.732	0.658**	1.91	2.98
RF	0.709	0.626**	2.17	3.22
This study	0.755	0.673**	1.67	2.71

Note: IDW, Inverse Distance Weight; SVM, Support Vector Machine; RF, Random Forest; PCC, Pearson Correlation Coefficient; RMSE, Root Mean Squared Error; MAE, Mean Absolute Error.

Different models tend to present great disparity in the prediction accuracy of SOC content between different soil depths (Batjes, 2016). Gomes et al. (2019) and Taguas et al. (2021) found that Random Forests (RF) have the best performance, compared with SVM (Support Vector Machines), Cubist, and GLM (Generalized Linear Models) in predicting SOC stocks at all depths (0–5, 5–15, 15–30, 30–60, and 60–100 cm) in Brazil. He et al. (2021a) showed that the prediction accuracy of SOC stocks in the soil leaching layer (0–30 cm) based on the digital soil mapping method (MAE = 1.29, and RMSE = 1.99) is lower than that of traditional prediction methods (MAE = 0.79, and RMSE = 0.94) in Jiyuan City, China. Hence, the application of predictive models should follow the principle of parsimony – Occam's razor – suggesting that the best model can explain the same phenomena using fewer variables without loss of performance (Castaldi et al., 2019; Guo et al., 2019). We argue that the selection of spatial prediction models should consider the balance between model prediction capability and training costs.

4.2. Influencing mechanisms of land-use changes on surface SOC stocks

Many studies have proved that land use types have different impacts on surface SOC stocks, and the conversions between land use types can modify the micro-ecological environment of the soil, thereby affecting the physical and chemical properties of the soil and affecting the distribution of soil aggregates (Abera et al., 2021; Al-Hanbali et al., 2021; Dvornikov et al., 2021). Taking the surface soil (0–30 cm) in this study area in 2019 as an example, the SOC content of cultivated land is the highest (0.64 kg/m^{-2}), while the SOC content of other land use types is ranked as follows: woodland (0.54 kg/m^{-2}) > grassland (0.53 kg/m^{-2}) > barren land (0.42 kg/m^{-2}) > construction land (0.37 kg/m^{-2}). The study carried out by Don et al. (2011) showed that the SOC of different land use types in the tropics follows: primary forest > secondary forest > grassland > cropland > perennial crops. The discrepancy of SOC stocks of land use types between our studies and previous studies can be attributed partially to (1) the different land use classification systems and (2) the different geographical locations of the investigated areas.

This study proves that land-use changes have a great contribution to SOC stocks. The expansion of construction land is the main cause of SOC loss. For example, the occupation of cultivated land by construction land caused a reduction of SOC by 4.54 Gg C, and the occupation of grassland by construction land caused a reduction of SOC by 4.77 Gg C. These results are partly consistent with existing efforts. For example, Jost et al. (2021) suggested that the temporal changes in SOC stocks led to the most rapid losses for land-use changes from grassland to cropland in the Mostviertel region. Similarly, Balkovic et al. (2020) found that land use change towards cropland negatively affects SOC stocks in Slovakia. We believe the inconsistency in findings can be explained by the study area discrepancies. For example, a large area of desertified sparse grassland is similar to barren land in our study area, leading to grassland soil not having great aggregate stability and microbial communities. Therefore, diverging conclusions might result from different analytical procedures and scales, assumptions on climate change, and other regional differences in natural and socio-economic drivers of SOC dynamics.

4.3. Advances in agricultural management practices are expected to increase the sequestration potential of surface SOC

In the process of analyzing the impact of land-use changes on surface SOC stocks, we noticed that the increase of SOC in “stable cultivated land” has the greatest contribution to SOC storage in the Sangong river basin. The results indicate the SOC of “stable cultivated land” increased by 36.0 Gg C from 2005 to 2019, accounting for 54.9% of the increase of SOC stocks in the study area. This result confirms that changes in farmland soil carbon pool can be adjusted for long-term or short-term through manual management. This study provides an important reference that supports the "four-thousandth plan" (Soussana et al., 2019) from the French Minister of Agriculture at the 21st United Nations Climate Change Conference. This plan states that the global SOC storage at a depth of 2 m increases by four thousandths every year, which can offset the global fossil fuel carbon emissions in that year; the global SOC storage of 1 m depth soil increases by four thousandths every year, which can offset the net carbon dioxide emissions that were deducted from the carbon sinks of terrestrial ecosystems and ocean carbonization in that year (Noulekoun et al., 2021). The proposal of this plan reflects the importance of the soil carbon pool in the global carbon cycle system, and its realization depends on the positive contribution of the agricultural soil carbon pool (Corbeels et al., 2019).

We guess that the contribution from “stable cultivated land” to SOC storage can be explained by the advances in agricultural management practices, a hot topic in the current research on SOC (Guevara et al., 2018; Jin et al., 2021). Our study indicates that film mulching, drip irrigation, and reducing the application of fertilizer application can have a positive impact on the SOC sequestration capacity. Existing efforts mostly focused on the impact of farming methods on SOC stocks in different study areas (Lavallee et al., 2020; Loke et al., 2021; Martinez-Mena et al., 2020). Despite these efforts, however, we indicate that investigations on the impact of agricultural management practices on SOC stocks are still insufficient, especially in arid regions. Agricultural management plans such as film mulching, drip irrigation, and the application of fertilizer should receive more attention, as they can gradually change the management model of arid agriculture and are expected to determine the future development of agriculture in arid areas.

5. Conclusion

In this study, we investigated the joint impact of land-use changes and agricultural management practices (i.e., film mulching, drip irrigation, and the application of fertilizer) on surface SOC stocks. We collected soil sample data to estimate surface SOC storage in the Sangong river basin in 2005 and 2019. We derived the spatiotemporal dynamics of SOC stocks and designed a conceptual framework to explore the positive or negative effects of land-use changes and agricultural management practices on surface SOC stocks. The spatiotemporal variations of estimation results indicate a huge jump in SOC stocks from 2005 (516 Gg C) to 2019 (582 Gg C). Land-use changes caused both positive and negative impacts on SOC storage dynamics: the conversion of cultivated land to grassland (+3 Gg C) also has a positive impact on SOC stocks, while the expansion of construction land led to a decline in SOC stocks by − 9.49 Gg C. The substantial increase in SOC stocks in stable cultivated land can be attributed to the advances in agricultural management practices. The results of this study suggest that short-term adjustments to agricultural carbon pools can effectively increase the carbon sequestration capacity at the regional scale. Our results are expected to benefit the “Carbon Neutrality” of China and planners in better managing agricultural land. Although the results of this study are specific to the Sangong river basin, the conceptual and methodological design in this study can be adapted to other regions to explore the impacts of land-use changes and agricultural management practices on SOC stocks.

Funding information

This work is supported by the National Natural Science Foundation of China under Grants 42090012 and 42205127; Sichuan Province Department of Science and Technology of China under Grants 2022YFN0031, 2023YFN0022, and 2023YFS0381; China Association for Science and Technology under Grant 20220615ZZ07110306.

Declaration of Competing Interest

The authors declare no conflict of interest. The founding sponsors had no role in the design of the study, in the collection, analyses, or interpretation of the data, in the writing of the manuscript, or in the decision to publish the results.

Data Availability

Data will be made available on request.

Acknowledgments

We would like to extend sincere gratitude to the academic editor and reviewers for their constructive comments which greatly helped us to improve the quality of this manuscript.

Appendix A. Supporting information

Supplementary data associated with this article can be found in the online version at doi:10.1016/j.still.2023.105716.

References

Abera, W., Tamene, L., Abegaz, A., Hailu, H., Piikki, K., Soderstrom, M., Girvetz, E., Sommer, R., 2021. Estimating spatially distributed SOC sequestration potentials of sustainable land management practices in Ethiopia. J. Environ. Manag. 286, 112191.

Al-Hanbali, A., Shibuta, K., Alsaaideh, B., Tawara, Y., 2021. Analysis of the land suitability for paddy fields in Tanzania using a GIS-based analytical hierarchy process. Geo-Spat. Inf. Sci. 25, 212–228.

Artemyeva, Z., Danchenko, N., Kolyagin, Y., Kirillova, N., Kogut, B., 2021. Chemical structure of soil organic matter and its role in aggregate formation in Haplic Chernozem under the contrasting land use variants. Catena 204, 105403.

Bai, Y., Sheng, M., Hu, Q., Zhao, C., Wu, J., Zhang, M., 2020. Effects of land use change on soil organic carbon and its components in karst rocky desertification of southwest China. J. Appl. Ecol. 31, 1607–1616.

Bai, Z., Caspari, T., Gonzalez, M.R., Batjes, N.H., Mader, P., Bunemann, E.K., de Goede, R., Brussaard, L., Xu, M., Ferreira, C.S.S., 2018. Effects of agricultural management practices on soil quality: a review of long-term experiments for Europe and China. Agric. Ecosyst. Environ. 265, 1–7.

Baker, J.M., Ochsner, T.E., Venterea, R.T., Griffis, T.J., 2007. Tillage and soil carbon sequestration - what do we really know? Agric. Ecosyst. Environ. 118, 1–5.

Balesdent, J., Basile-Doelsch, I., Chadoeuf, J., Cornu, S., Derrien, D., Fekiacova, Z., Hatte, C., 2018. Atmosphere-soil carbon transfer as a function of soil depth. Nature 559, 599.

Balkovic, J., Madaras, M., Skalsky, R., Folberth, C., Smatanova, M., Schmid, E., van der Velde, M., Kraxner, F., Obersteiner, M., 2020. Verifiable soil organic carbon modelling to facilitate regional reporting of cropland carbon change: a test case in the Czech Republic. J. Environ. Manag. 274, 111206.

Batjes, N.H., 2016. Harmonized soil property values for broad-scale modelling (WISE30sec) with estimates of global soil carbon stocks. Geoderma 269, 61–68.

Bouasria, A., Namr, K.I., Rahimi, A., Ettachfini, E., Rerhou, B., 2022. Evaluation of Landsat 8 image pansharpening in estimating soil organic matter using multiple linear regression and artificial neural networks. Geo-Spat. Inf. Sci. 25, 353–364.

Bradford, M.A., Wieder, W.R., Bonan, G.B., Fierer, N., Raymond, P.A., Crowther, T.W., 2016. Managing uncertainty in soil carbon feedbacks to climate change. Nat. Clim. Change 6, 751–758.

Carvalhais, N., Forkel, M., Khomik, M., Bellarby, J., Jung, M., Migliavacca, M., Mu, M.Q., Saatchi, S., Santoro, M., Thurner, M., 2014. Global covariation of carbon turnover times with climate in terrestrial ecosystems. Nature 514, 213.

Castaldi, F., Hueni, A., Chabrillat, S., Ward, K., Buttafuoco, G., Bomans, B., Vreys, K., Brell, M., van Wesemael, B., 2019. Evaluating the capability of the Sentinel 2 data for soil organic carbon prediction in croplands. ISPRS J. Photogramm. Remote Sens. 147, 267–282.

Cooper, H.V., Sjogersten, S., Lark, R.M., Girkin, N.T., Vane, C.H., Calonego, J.C., Rosolem, C., Mooney, S.J., 2021. Long-term zero-tillage enhances the protection of soil carbon in tropical agriculture. Eur. J. Soil Sci. 72, 2477–2492.

Corbeels, M., Cardinael, R., Naudin, K., Guibert, H., Torquebiau, E., 2019. The 4 per 1000 goal and soil carbon storage under agroforestry and conservation agriculture systems in sub-Saharan Africa. Soil Tillage Res. 188, 16–26.
Crystal-Ornelas, R., Thapa, R., Tully, K.L., 2021. Soil organic carbon is affected by organic amendments, conservation tillage, and cover cropping in organic farming systems: a meta-analysis. Agric. Ecosyst. Environ. 312, 107356.
Damian, J.M., Durigan, M.R., Cherubin, M.R., Maia, S.M.F., Ogle, S.M., de Camargo, P.B., Ferreira, J.N., de Oliveira, R.C., Cerri, C.E.P., 2021. Deforestation and land use change mediate soil carbon changes in the eastern Brazilian Amazon. Reg. Environ. Change 21, 64.
Dignac, M.F., Derrien, D., Barre, P., Barot, S., Cecillon, L., Chenu, C., Chevallier, T., Freschet, G.T., Garnier, P., Guenet, B., Hedde, M., Klumpp, K., Lashermes, G., Maron, P.A., Nunan, N., Roumet, C., Basile-Doelsch, I., 2017. Increasing soil carbon storage: mechanisms, effects of agricultural practices and proxies. A review. Agron. Sustain. Dev. 37, 14.
Dlamini, P., Chivenge, P., Chaplot, V., 2016. Overgrazing decreases soil organic carbon stocks the most under dry climates and low soil pH: A meta-analysis shows. Agric. Ecosyst. Environ. 221, 258–269.
Don, A., Schumacher, J., Freibauer, A., 2011. Impact of tropical land-use change on soil organic carbon stocks - a meta-analysis. Glob. Change Biol. 17, 1658–1670.
Dvornikov, Y.A., Vasenev, V.I., Romzaykina, O.N., Grigorieva, V.E., Litvinov, Y.A., Gorbov, S.N., Dolgikh, A.V., Korneykova, M.V., Gosse, D.D., 2021. Projecting the urbanization effect on soil organic carbon stocks in polar and steppe areas of European Russia by remote sensing. Geoderma 399, 115039.
Franco, A.L.C., Cherubin, M.R., Cerri, C.E.P., Six, J., Wall, D.H., Cerri, C.C., 2020. Linking soil engineers, structural stability, and organic matter allocation to unravel soil carbon responses to land-use change. Soil Biol. Biochem. 150, 107998.
Fu, X., Wang, J., Liu, Q., Li, R., 2015. Soil aggregate and organic carbon contents with different surface mulching under dryland farming system. J. Plant Nutr. Fertil. 21, 1423–1430.
Fujisaki, K., Perrin, A.S., Desjardins, T., Bernoux, M., Balbino, L.C., Brossard, M., 2015. From forest to cropland and pasture systems: a critical review of soil organic carbon stocks changes in Amazonia. Glob. Change Biol. 21, 2773–2786.
Gomes, L.C., Faria, R.M., de Souza, E., Veloso, G.V., Schaefer, C.E.G.R., Fernandes, E.I., 2019. Modelling and mapping soil organic carbon stocks in Brazil. Geoderma 340, 337–350.
Guevara, M., Olmedo, G.F., Stell, E., et al., 2018. No silver bullet for digital soil mapping: country-specific soil organic carbon estimates across Latin America. Soil 4, 173–193.
Guo, L., Zhang, h, Shi, T., Chen, Y., Jiang, Q., Linderman, M., 2019. Prediction of soil organic carbon stock by laboratory spectral data and airborne hyperspectral images. Geoderma 337, 32–41.
Guo, L., Sun, X., Fu, P., Shi, T., Dang, L., Chen, Y., Linderman, M., Zhang, G., Zhang, Y., Jiang, Q., 2021. Mapping soil organic carbon stock by hyperspectral and time-series multispectral remote sensing images in low-relief agricultural areas. Geoderma 398, 115118.
He, L., Liu, Q., Wang, D., Zhang, Z., Xu, C., Shi, M., 2021a. Estimation of soil organic carbon storage based on digital soil mapping technique. J. Appl. Ecol. 32, 591–600.
He, L., Lu, S., Wang, G., Mu, J., Zhang, Y., Wang, X., 2021b. Changes in soil organic carbon fractions and enzyme activities in response to tillage practices in the Loess Plateau of China. Soil Tillage Res. 209, 104940.
Hou, Y., Zhang, X., Tang, H., 2011. Grey relation study between land transfer factors and land transfer size of the Sangong River Basin. Arid Land Geogr. 34, 1024–1031.
Huang, A., Yang, L., Du, T., Zhang, B., Song, Y., Wang, A., Qin, J., 2015. Spatial distribution of the soil organic matter based on multiple soil factors. Arid Land Geogr. 38, 994–1003.
Jiang, S., 2019. Review on soil bulk density determination method. Hubei Agric. Sci. 58, 82–86.
Jin, V.L., Wienhold, B.J., Mikha, M.M., Schmer, M.R., 2021. Cropping system partially offsets tillage-related degradation of soil organic carbon and aggregate properties in a 30-yr rainfed agroecosystem. Soil Tillage Res. 209, 104968.
Jost, E., Schonhart, M., Skalsky, R., Balkovic, J., Schmid, E., Mitter, H., 2021. Dynamic soil functions assessment employing land use and climate scenarios at regional scale. J. Environ. Manag. 287, 112318.
Keskin, H., Grunwald, S., Harris, W.G., 2019. Digital mapping of soil carbon fractions with machine learning. Geoderma 339, 40–58.
Lal, R., 2018. Digging deeper: a holistic perspective of factors affecting soil organic carbon sequestration in agroecosystems. Glob. Change Biol. 24, 3285–3301.
Lavallee, J.M., Soong, J.L., Cotrufo, M.F., 2020. Conceptualizing soil organic matter into particulate and mineral-associated forms to address global change in the 21st century. Glob. Change Biol. 26, 261–273.
Lemma, B., Williams, S., Paustian, K., 2021. Long term soil carbon sequestration potential of smallholder croplands in southern Ethiopia with DAYCENT model. J. Environ. Manag. 294, 112893.
Li, Z., Jiao, L., Zhang, B., Xu, G., Liu, J., 2021. Understanding the pattern and mechanism of spatial concentration of urban land use, population and economic activities: a case study in Wuhan, China. Geo-Spat. Inf. Sci. 24, 678–694.
Li, R., Zheng, S., Duan, C., Wang, L., Zhang, C., 2022. Land cover classification from remote sensing images based on multi-scale fully convolutional network. Geo-Spat. Inf. Sci. 25, 278-294. 25, 278–294.
Liu, M., Han, G., Zhang, Q., 2020. Effects of agricultural abandonment on soil aggregation, soil organic carbon storage and stabilization: Results from observation in a small karst catchment, Southwest China. Agric. Ecosyst. Environ. 288, 106719.
Lizaga, I., Quijano, L., Gaspar, L., Ramos, M.C., Navas, A., 2019. Linking land use changes to variation in soil properties in a Mediterranean mountain agroecosystem. Catena 172, 516–527.
Loke, P.F., Schimper, J.J., Kotze, E., du Preez, C.C., 2021. Long-term wheat production management effects on soil fertility indicators in the semi-arid eastern Free State, South Africa. South Afr. J. Plant Soil. 38, 93–106.
Martinez-Mena, M., Carrillo-Lopez, E., Boix-Fayos, C., Almagro, M., Franco, N.G., Diaz-Pereira, E., Montoya, I., de Vente, J., 2020. Long-term effectiveness of sustainable land management practices to control runoff, soil erosion, and nutrient loss and the role of rainfall intensity in Mediterranean rainfed agroecosystems. Catena 187, 104352.
Mazzoncini, M., Sapkota, T.B., Barberi, P., Antichi, D., Risaliti, Rosalba, 2011. Long-term effect of tillage, nitrogen fertilization and cover crops on soil organic carbon and total nitrogen content. Soil Tillage Res. 114, 165–174.
Mbuthia, L.W., Acosta-Martinez, V., DeBruyn, J., Schaeffer, S., Tyler, D., Odoi, E., Mpheshea, M., Walker, F., Eash, N., 2015. Long term tillage, cover crop, and fertilization effects on microbial community structure, activity: Implications for soil quality. Soil Biol. Biochem. 89, 24–34.
Ming, G., Hu, H., Tian, F., Khan, M.Y.A., Zhang, Q., 2021. Carbon budget for a plastic-film mulched and drip-irrigated cotton field in an oasis of Northwest China. Agric. For. Meteorol. 306, 108447.
Morais, V.A., Ferreira, G.W.D., de Mello, J.M., Silva, C.A., de Mello, C.R., Araujo, E.J.G., David, H.C., da Silva, A.C., Scolforo, J.R.S., 2020. Spatial distribution of soil carbon stocks in the Cerrado biome of Minas Gerais. Braz. Catena 185, 104285.
Nabiollahi, K., Golmohamadi, F., Taghizadeh-Mehrjardi, R., Kerry, R., Davari, M., 2018. Assessing the effects of slope gradient and land use change on soil quality degradation through digital mapping of soil quality indices and soil loss rate. Geoderma 318, 16–28.
Nandan, R., Singh, V., Singh, S.S., Kumar, V., Hazra, K.K., Nath, C.P., Poonia, S., Malik, R.K., Bhattacharyya, R., McDonald, A., 2019. Impact of conservation tillage in rice-based cropping systems on soil aggregation, carbon pools and nutrients. Geoderma 340, 104–114.
Nocita, M., Stevens, A., Toth, G., Panagos, P., van-Wesemael, B., Montanarella, L., 2014. Prediction of soil organic carbon content by diffuse reflectance spectroscopy using a local partial least square regression approach. Soil Biol. Biochem. 68, 337–347.
Noulekoun, F., Birhane, E., Kassa, H., Berhe, A., Gebremichael, Z.M., Adem, N.M., Syoum, Y., Mengistu, T., Lemma, B., Hagazi, N., Abrha, H., Rannestad, M.M., Mensah, S., 2021. Grazing exclosures increase soil organic carbon stock at a rate greater than "4 per 1000" per year across agricultural landscapes in Northern Ethiopia. Sci. Total Environ. 782, 146821.
Qiu, X., Cao, G., Zhang, Z., Zhao, M., He, Q., Cheng, M., Gao, S., 2022. Vertical distribution characteristics of soil organic carbon and total nitrogen density in alpine farmland and their relationships with altitude. Chin. J. Soil Sci. 53, 623–630.
Ramirez, P.B., Fuentes-Alburquenque, S., Diez, B., Vargas, I., Bonilla, C.A., 2020. Soil microbial community responses to labile organic carbon fractions in relation to soil type and land use along a climate gradient. Soil Biol. Biochem. 141, 107692.
Ren, R., Du, Z., Sun, Y., Song, X., Lu, S., 2020. Soil aggregate and its organic carbon distribution characteristics at different land use patterns in hilly areas of north China. Acta Ecol. Sin. 40, 6991–6999.
Sanaullah, M., Usman, M., Wakeel, A., Cheema, S.A., Ashraf, I., Farooq, M., 2020. Terrestrial ecosystem functioning affected by agricultural management systems: a review. Soil Tillage Res. 196, 104464.
Sanderman, J., Hengl, T., Fiske, G.J., 2017. Soil carbon debt of 12,000 years of human land use. Proc. Natl. Acad. Sci. USA 114, 9575–9580.
Shi, C., Xu, M., Qiu, Y., 2016. Estimation of topsoil carbon sequestration potential of cropland through different methods: a case study in Zhuanglang County, Gansu Province. Huan jing ke xue 37, 1098–1105.
Soussana, J.F., Lutfalla, S., Ehrhardt, F., Rosenstock, T., Lamanna, C., Havlik, P., Havlik, P., Wollenberg, E., Chotte, J.L., Torquebiau, E., Ciais, P., Smith, P., Lal, R., 2019. Matching policy and science: Rationale for the '4 per 1000-soils for food security and climate' initiative. Soil Tillage Res. 188, SI3–SI15.
Taguas, E.V., Bingner, R.L., Momm, H.G., Wells, R., Locke, M.A., 2021. Modelling scenarios of soil properties and managements in olive groves at the micro-catchment scale with the AnnAGNPS model to quantify organic carbon. Catena 203, 105333.
Wang, Y., Zhao, P., 2020. Effect of land use types on stability of soil aggregates,soil organic carbon fractions and soil respiration in Northern China. Res. Soil Water Conserv. 27, 59–65.
Wiesmeier, M., Urbanski, L., Hobley, E., Lang, B., von Lutzow, M., Marin-Spiotta, E., van Wesemael, B., Rabot, E., Liess, M., Garcia-Franco, N., Wollschlager, U., Vogel, H.J., Kogel-Knabner, I., 2019. Soil organic carbon storage as a key function of soils - A review of drivers and indicators at various scales. Geoderma 333, 149–162.
Wu, Z., Liu, Y., Chen, Y., Guo, L., Jiang, Q., Wang, S., 2018. Spatial interpolation model of soil organic carbon density considering land-use and spatial heterogeneity. Chin. J. Appl. Ecol. 29, 238–246.
Xiao, H., Shi, Z., Li, Z., Chen, J., Huang, B., Yue, Z., Zhan, Y., 2021. The regulatory effects of biotic and abiotic factors on soil respiration under different land-use types. Ecol. Indic. 127, 107787.
Xie, Z., Zhu, J., Liu, G., Cadissh, G., Hasegawa, T., Chen, C., Sun, H., Tang, H., Zeng, Q., 2007. Soil organic carbon stocks in China and changes from 1980s to 2000s. Glob. Change Biol. 13, 1989–2007.
Xu, N., Zhang, T., Wang, X., Liu, H., 2011. Soil organic carbon storage changes in Yangtze Delta region, China. Environ. Earth Sci. 63, 1021–1028.
Xu, X., Zhang, D., Liu, X., Ou, J., Wu, X., 2022. Simulating multiple urban land use changes by integrating transportation accessibility and a vector-based cellular automata: a case study on city of Toronto. Geo-Spat. Inf. Sci. 25, 439–456.
Yang, K., Xie, H., Sui, B., Zhou, Q., Liu, P., Wang, H., 2020. Research on Spatial Interpolation of Rainfall Based on GIS-A Case Study of Hunan Province. Res. Soil Water Conserv. 27, 134–138, 145.

Zhang, X., Li, X., Ji, X., Zhang, Z., Zhang, H., Zha, T., Jiang, L., 2021. Elevation and total nitrogen are the critical factors that control the spatial distribution of soil organic carbon content in the shrubland on the Bashang Plateau. China. Catena 204, 105415.
Zhang, Z., Ding, J., Wang, J., Ge, X., Wang, J., Tian, M., Zhao, Q., 2020. Digital soil properties mapping by ensembling soil-environment relationship and machine learning in arid regions. Sci. Agric. Sin. 53, 563–573.
Zhao, Z., Gao, S., Lu, C., Li, X., Li, F., Wang, T., 2021. Effects of different tillage and fertilization management practices on soil organic carbon and aggregates under the rice-wheat rotation system. Soil Tillage Res. 212, 105071.
Zhuang, Q., Shao, Z., Li, D., Huang, X., Altan, O., Wu, S., 2022a. Isolating the direct and indirect impacts of urbanization on vegetation carbon sequestration capacity in a large oasis city: evidence from Urumqi, China. Geo-Spat. Inf. Sci. https://doi.org/10.1080/10095020.2022.2118624.
Zhuang, Q., Shao, Z., Li, D., Huang, X., Cai, B., Altan, O., Wu, S., 2022b. Unequal weakening of urbanization and soil salinization on vegetation production capacity. Geoderma. 411, 115712.